RAA 2021 Vol. **21** No. **4**, 88(5pp) doi: 10.1088/1674-4527/21/4/88

http://www.raa-journal.org *http://iopscience.iop.org/raa*

Research in Astronomy and Astrophysics

Design of the cryogenic system of the wideband phased array feed for QTT

Jun Ma, Yang Wu, Song Xiao, Sheng-Pu Niu and Kai Wang

Xinjiang Astronomical Observatory, Chinese Academy of Sciences, Urumqi 830011, China; *majun@xao.ac.cn*

Received 2020 July 26; accepted 2020 September 27

Abstract Phased array feeds (PAFs), which illuminate the dish with digitally synthesized beams instead of separated horns, provide the capability for wider and continuous field-of-view surveys. As a promising technology for next generation radio telescopes, PAFs will provide the Qi Tai Telescope (QTT), which will be next world-class fully steerable radio telescope, an opportunity of reaching several cutting-edge science goals. This paper presents a brief introduction of the wideband PAF for QTT, and the detailed design and simulation of the cryogenic system. Based on this design, a scaled prototype of the spherical vacuum window, which is the key part of the cryogenic system, has been built and the performance is verified.

Key words: Phased Array Feed — Vacuum window — Cryo — telescope

1 INTRODUCTION

The Qi Tai Telescope (QTT), which aims to be a fully steerable radio telescope of 110m aperture in diameter, will play an important role among the world-class scientific facilities (Xu & Wang 2016). To explore the fundamental research areas in radio astronomy, such as pulsars, molecular spectral lines, and VLBI observations, sets of receivers are employed to cover a wide frequency band from 270 MHz to 115 GHz. Since the research in low band is crucial for a number of significant science goals of QTT, two types of advanced receivers are under development. One is quad-ridged flared horn (QRFH) to reach ultra-wide operating bandwidth, another is phased array feed (PAF) to realize a wide field of view and higher survey speed.

This paper presents the overall scheme of the PAF designed for QTT, especially the details of the cryogenic system. As the key part and innovation of this cryogenic system, a prototype of the spherical vacuum window is built and measured, the results are given and compared with simulations.

2 ARRAY SPECIFICATIONS AND CONFIGURATION

Preliminary performance requirements for the PAF on QTT are shown in Table 1. The goal is to build a PAF of more than 100 array elements in each polarization, covering an operating frequency range of 0.7–1.8 GHz, and instantaneous bandwidth around 500 MHz. Both the array and the low noise amplifiers (LNAs) will be cooled to improve the system sensitivity.

To meet the operating frequency range, the Vivaldi antenna is selected to be the array element. Firstly, the focal field distributions are calculated at 0.70 GHz, 1.25 GHz and 1.80 GHz with Half Power Beam Width (HPBW) interval incident planner waves, using a joint method of physical optics and physical theory of diffraction[1], and the results are shown in Figure 1. From Figure 1, the numbers of effectively simultaneous beams to synthesize can be determined by the array aperture and focal field distribution. Assuming a plane waves at 1.8 GHz incidents from boresign and near the offset angle, the number and spacing of the array element is optimized to match this field distribution, and the results show a 6-by-5 array for one beam is necessary to achieve the requirement on aperture efficiency.

The preliminary specifications of PAF for QTT are shown in Table 1.

3 DESIGN OF THE CRYOGENIC SYSTEM

3.1 Overview

Cryogenic cooling is an effective way to reduce the thermal noise that comes from feed assembly and LNA, improving the sensitivity of a receiving system (Gawande et al. 2014; Martellosio et al. 2016; Cortes-Medellin et al. 2014). In the areas of radio astronomy and deep space exploration,

[1] *https://www.ticra.com/software/grasp/*

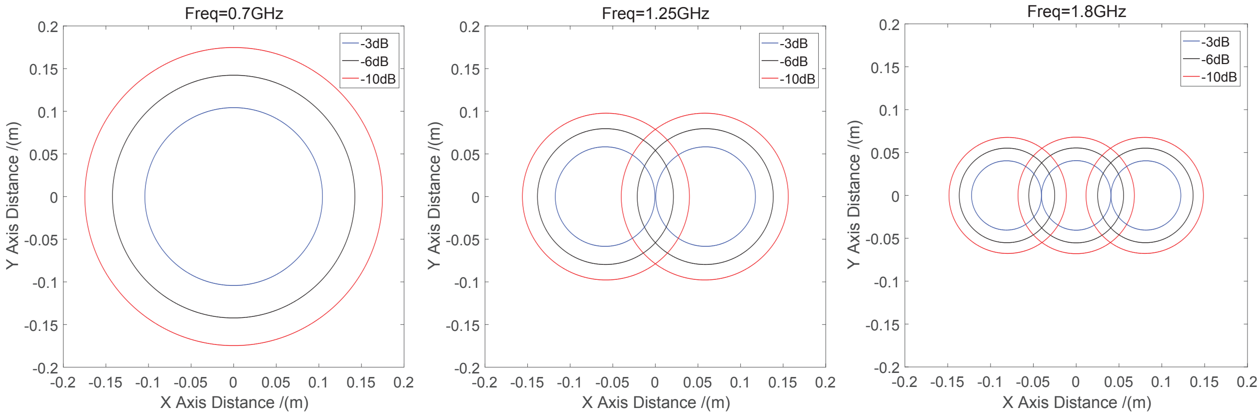

Fig. 1 Diagram of QTT focal field caused by plane waves incident in different directions.

Table 1 Performance Specifications for QTT PAF

Parameter	Quantity
Operating frequency range	0.7 ∼1.8 GHz
Instantaneous bandwidth	$\geq$ 500 MHz
Effective f/D	0.33
Field of view	0.2 *0.2 deg^2
Simultaneous beams	1@0.7 GHz
	4@1.2 GHz
	9@1.8 GHz
System noise temperature	25 K
Aperture efficiency	$\geq$ 60%
Cooling	Array and LNAs

since the dish has been too large for further aperture extension, cooled receivers are widely used for economically realizing the lower signal detecting limit.

Figure 2 shows the sectional drawing of the whole PAF designed for QTT. The PAF is 320 mm in height and 550 mm in diameter. The feeding array, of which there are 98 Vivaldi antennas in each polarization, 196 elements are arranged in a square configuration in total. Both the feeding array and the LNAs are connected to a copper ground plane and cooled. In the near future, a new design will be carried out, in which each Vivaldi element and its corresponding LNA is integrated together for less insertion loss and more compact. A spherical radome of 500 mm is employed to keep the PAF isolated from the air while remaining transparent to electromagnetic waves, coinciding the center of the sphere with the phase center of the feeding array.

A layer of Mylar will cover the feeding array to reduce the thermal load from ambient.

3.2 Vacuum Window

To effectively keeping the receiver in low temperature, a vacuum environment is necessary. The vacuum window, which is used for isolating the receiver from ambient, should be not only stiff enough to stand the atmosphere pressure, but also transparent to the electromagnetic wave, i.e. letting the wave pass with very low insertion loss and reflection (Beaudin et al. 1977; Schröder et al. 2016). The latter indicates that the material of the vacuum window should be: small in tangent of loss angle, close to the air in the relative dielectric constant, and thin in thickness. Traditional flat vacuum window is easy to build, but brings a metal flange around the aperture of the feed. This flange distorts the radiation pattern of the feed inevitably, degrading the radiation pattern of the dish and sensitivity of the telescope inevitably. To avoid this effect, a bigger flange is employed, leading to an increment in thermal load and more power consumption. As a result, a new-type vacuum window of spherical shape is studied to minimize the negative effects in this cryogenic system design. The advantage of this spherical vacuum window is that, the installation flange can be designed to be behind the aperture of the array. In this way, the flange-caused radiation pattern deformation is minimized.

Taking the electrical and mechanical characteristics of the material in account, as well as its availability, polymethyl methacrylate (PMMA), with Poisson's ratio of 0.32 and elasticity modulus of 3.16 GPa, is selected to build the first vacuum window prototype. The measured relative dielectric constant and tangent of loss angle of PMMA are 2.75 and 0.006 respectively, and they are reasonably constant with frequency in a wide range (Ma et al. 2018).

To determine the thickness of the vacuum window, finite element analysis (FEA) is carried out. Fixing the diameter of the sphere as designed 500 mm, the vacuum window thickness is parameterized and swept from 3 mm to 10 mm. The simulation results are shown in Figure 3 and Table 2.

Based on the simulation results, the margin of safety variance with thickness is calculated by the following function:

$$MS = \frac{\sigma_s}{f \times \sigma_{\max}} - 1\,, \tag{1}$$

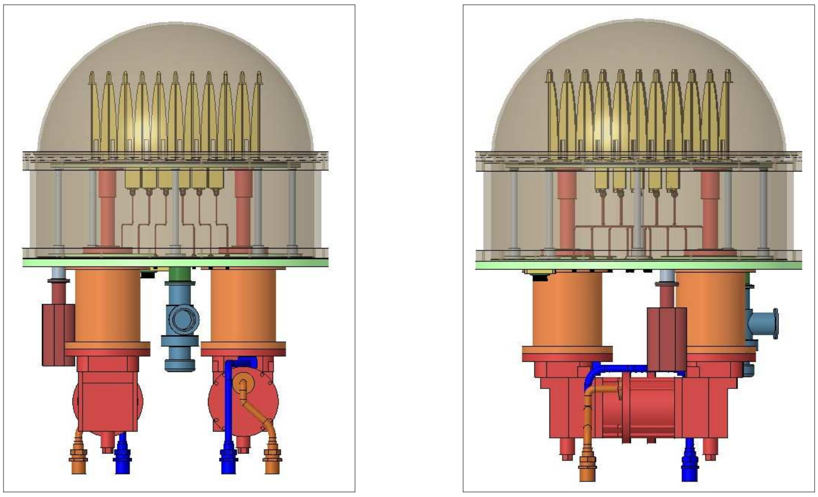

Fig. 2 Sectional drawing of the PAF.

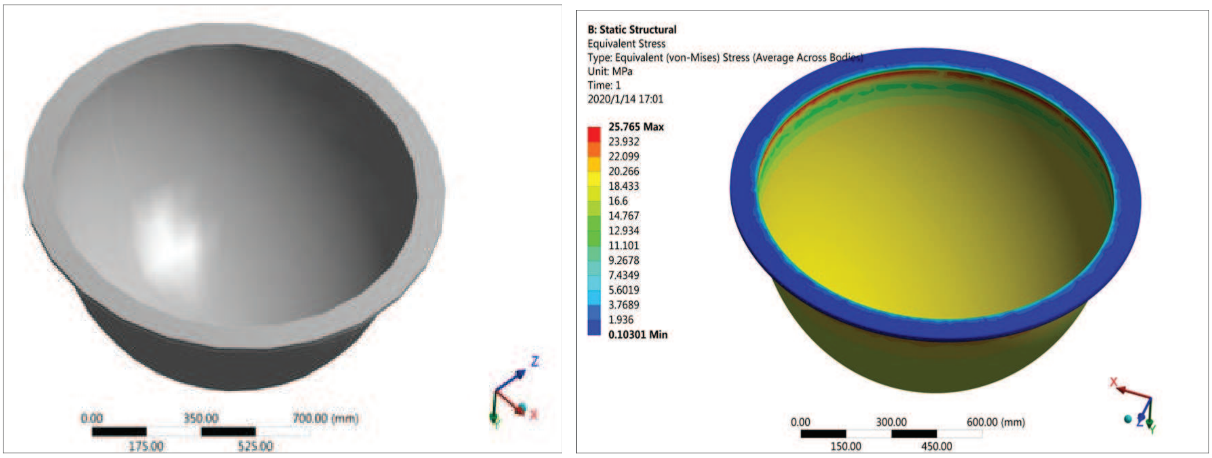

Fig. 3 FEA model and simulation result of the vacuum window.

Table 2 Estimate Stress And Margin Of Safety

Thickness	Stress (MPa)	Margin of Safety
3 mm	31.559	0.16
4 mm	25.765	0.42
6 mm	19.021	0.93
8 mm	14.922	1.46
10 mm	12.034	2.05

where MS is the margin of safety, σ_s is the allowable stress of material, $\sigma_{\max}$ is the maximum stress in use, and f is the safety factor which is set to be 1.5.

Considering the allowable stress σ_s of PMMA is 55 MPa, the vacuum window of 3 mm thickness can meet the strength.

Since the relative dielectric constant of the vacuum window cannot be identical with the air, reflecting a fraction of the wave from both sides, the voltage standing wave ratio (VSWR) of each Vivaldi element varies. Moreover, cause by the refraction of the vacuum window, the radiation pattern also slightly changes. So the sensitivity degradation in performance should be evaluated carefully.

4 SIMULATION AND MEASUREMENT RESULT

4.1 Figure of Merit Estimation

Given a noise temperature of 3 K in a cryogenic environment, which is realizable with current technology of low noise amplifier, the estimated sensitivity of each beam is shown in Figure 4.

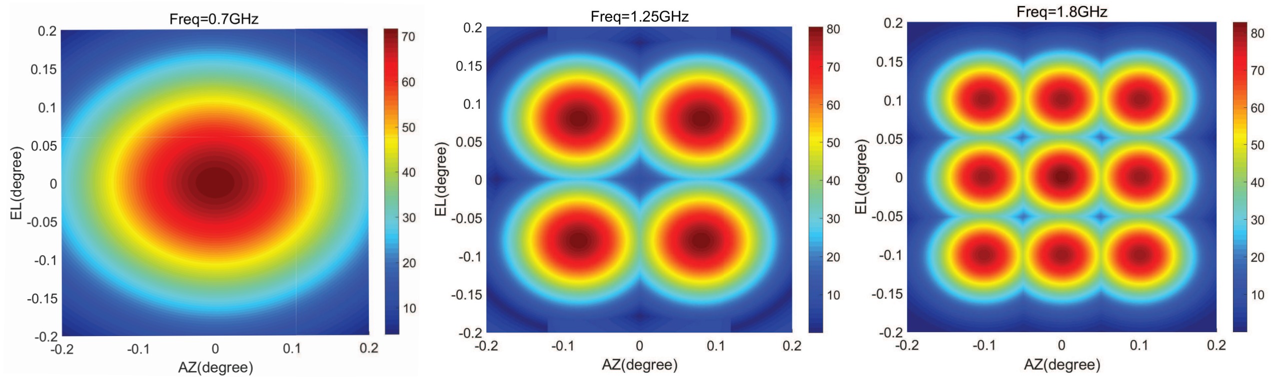

Fig. 4 Sensitivity variance over beam scan angle with number of elements per beam.

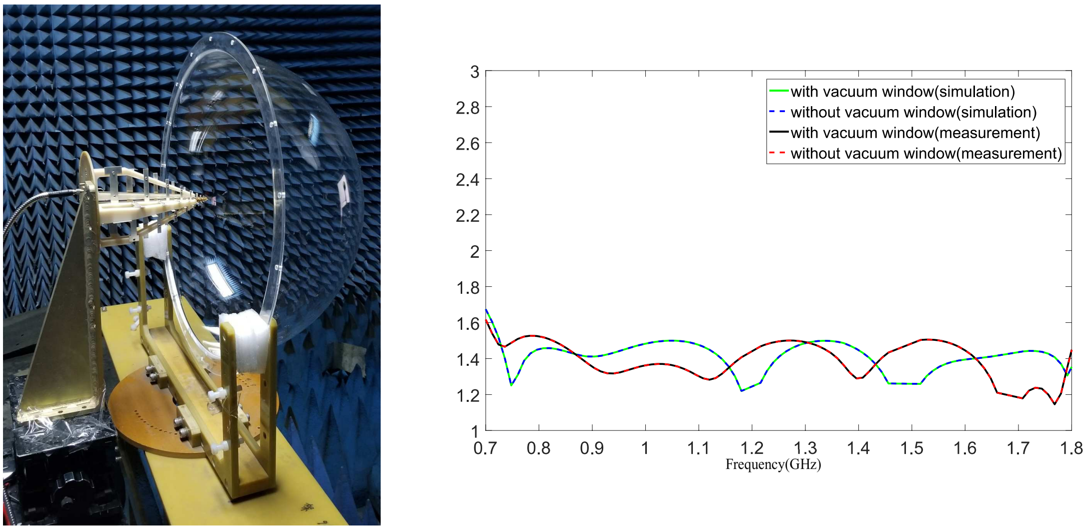

Fig. 5 Photograph and results of VSWR measurements.

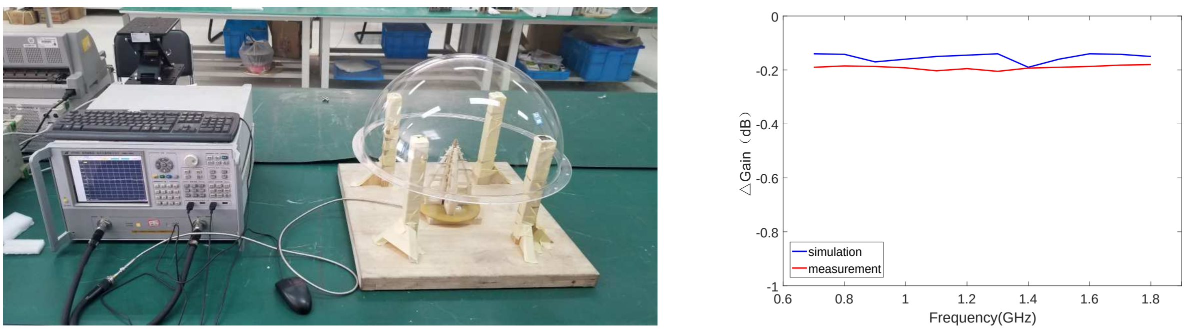

Fig. 6 Gain difference caused by the vacuum window.

4.2 Vacuum Window Prototype Verification

Figure 5 shows the photograph and the results of VSWR measurement in conditions with/without the vacuum window, which indicates the vacuum window leads to a negligible VSWR increment from 0.7 GHz to 1.8 GHz.

According the result of electrical performance evaluation and FEA simulation, a vacuum window prototype of 3mm thickness is built and tested in anechoic chamber, the photograph during the test and the results are shown in Figure 6. From Figure 6, a reasonably good agreement between simulation and measurement is seen.

By integrating into an existed Dewar, the mechanical performance of the vacuum window prototype is tested. As is shown in Figure 7, this vacuum window works well and a vacuum degree of 5.2–3 Torr is achieved.

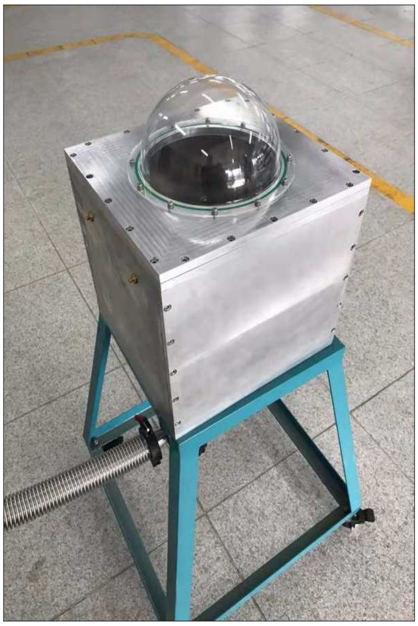

Fig. 7 The vacuum window under test.

5 CONCLUSIONS

A design scheme of the wideband PAF for the QTT is presented in this paper. Details of the cryogenic system are introduced, especially the development of the new-type vacuum window. The test results of the vacuum window prototype show its good RF performance as well as mechanical stiffness, and the agreement between simulation and measurement offers a supporting for the PAF building and further development.

Acknowledgements This work is supported by the Open Foundation of Key Laboratory of Xinjiang Uygur Autonomous Region (Grant No. 2017D04013).

References

Beaudin, G., Lazareff, B., & Mahieu, J. 1977, 7th European Microwave Conference. Copenhagen, 432

Cortes-Medellin, G., Viswash, A., Parsley, S., et al. 2014, Radio Science Meeting (Joint with AP-S Symposium), 2014 USNC-URSI. Beijing, 44, August, 2014.

Gawande, R., Bradley, R., & Langston, G. 2014, Rev. Sci. Instrum., 85, 104710

Ma, J., Xie, L., Wu ,Y., et al. 2018, 12th International Symposium on Antennas, Propagation and EM Theory, ISAPE 2018. Hangzhou, China, December 2018.

Martellosio, A., Pasian, M., Rayet, R., Rawson, S., & Bonhoure, T. 2016, 10th European Conference on Antennas and Propagation (EuCAP). Davos, 1

Schröder, A., Murk, A., Yagoubov, P., & Patt, F. 2016, IEEE Transactions on Terahertz Science and Technology, 6, 156

Xu, Q., & Wang, N. 2016, Progress in Astronomy, 34, 63 (in Chinese)